Accepted Manuscript

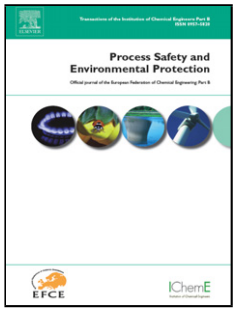

Title: Efficient removal of coomassie brilliant blue R-250 dye using starch/poly(alginic acid-*cl*-acrylamide) nanohydrogel

Authors: Gaurav Sharma, Mu. Naushad, Amit Kumar, Shailja Rana, Shweta Sharma, Amit Bhatnagar, Florian J. Stadler, Ayman A. Ghfar, Mohammad Rizwan Khan

PII: S0957-5820(17)30128-3
DOI: http://dx.doi.org/doi:10.1016/j.psep.2017.04.011
Reference: PSEP 1041

To appear in: *Process Safety and Environment Protection*

Received date: 20-12-2016
Revised date: 23-3-2017
Accepted date: 10-4-2017

Please cite this article as: Sharma, Gaurav, Naushad, Mu., Kumar, Amit, Rana, Shailja, Sharma, Shweta, Bhatnagar, Amit, J.Stadler, Florian, Ghfar, Ayman A., Khan, Mohammad Rizwan, Efficient removal of coomassie brilliant blue R-250 dye using starch/poly(alginic acid-cl-acrylamide) nanohydrogel.Process Safety and Environment Protection http://dx.doi.org/10.1016/j.psep.2017.04.011

Efficient removal of coomassie brilliant blue R-250 dye using starch/poly(alginic acid-*cl*-acrylamide) nanohydrogel

Gaurav Sharma[1], Mu. Naushad*[2], Amit Kumar[1], Shailja Rana[1], Shweta Sharma[1], Amit Bhatnagar[3], Florian J. Stadler[4], Ayman A. Ghfar[2], Mohammad Rizwan Khan[2]

[1]School of Chemistry, Shoolini University, Solan 173212, Himachal Pradesh, India

[2]Department of Chemistry, College of Science, Bld.#5, King Saud University, Riyadh, Saudi Arabia

[3]Department of Environmental and Biological Sciences, University of Eastern Finland, P.O. Box 1627, FI-70211 Kuopio, Finland

[4]College of Materials Science and Engineering, Shenzhen Key Laboratory of Polymer Science and Technology, Guangdong Research Center for Interfacial Engineering of Functional Materials, Nanshan District Key Lab for Biopolymers and Safety Evaluation, Shenzhen University, Shenzhen 518060, PR China

*Corresponding address: E-mail: mnaushad@ksu.edu.sa; Tel.: +91-9418807170

Graphical abstract

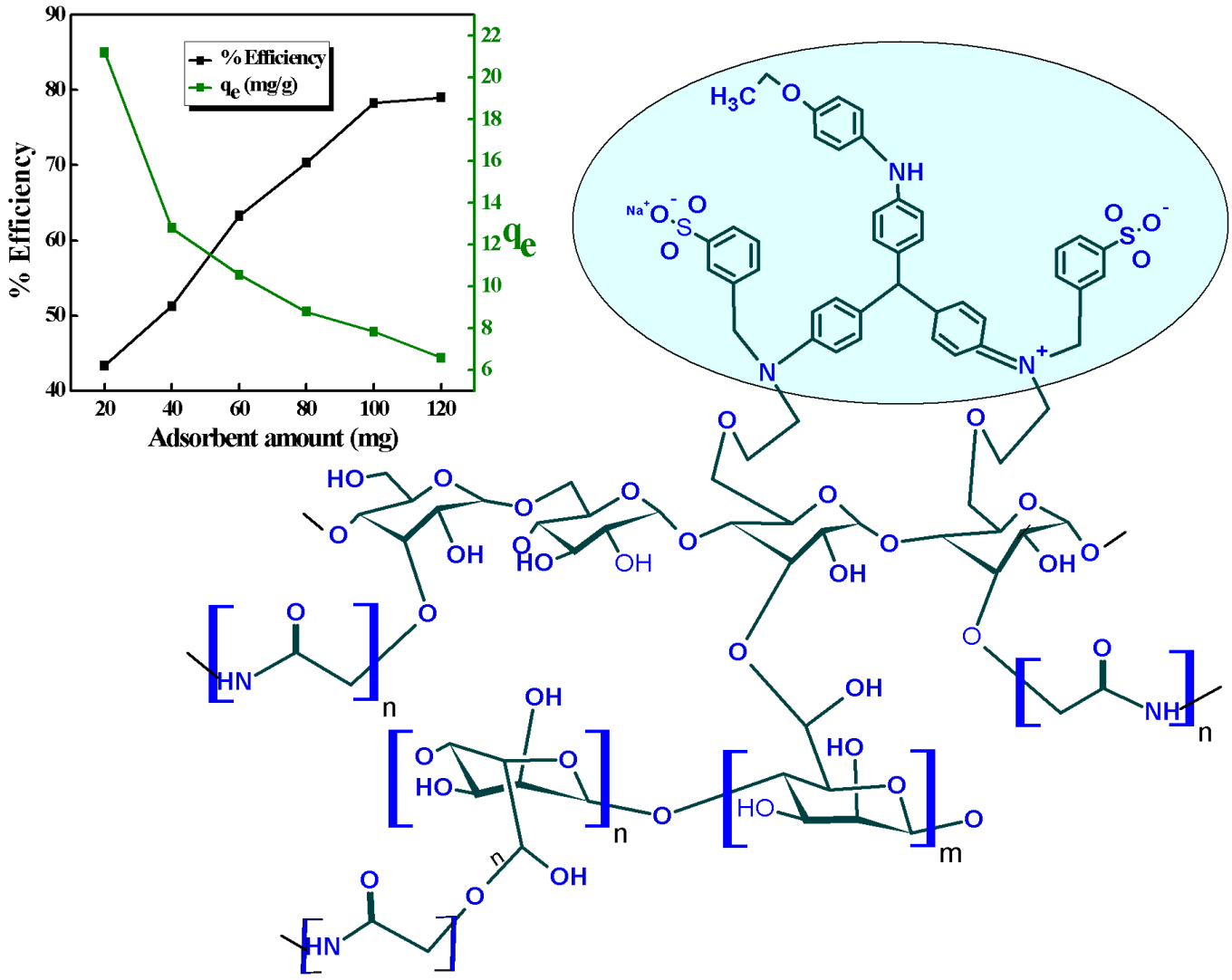

Adsorption of coomassie brilliant blue R-250 on Starch/Poly(alginic acid -cl- acrylamide)

Highlights

[1]. Starch/Poly(alginic acid-*cl*-acrylamide) have been synthesized by co-polymerization method

[2]. The efficacy of the prepared nanohydrogel has been studied for the removal of coomassie brilliant blue R-250 from the aqueous solution

[3]. The optimum pH for the adsorption of the CB dye was found 5

[4]. The adsorption of CB was endothermic and spontaneous in nature

Abstract:

In this study, we have synthesized a starch/poly(alginic acid-*cl*-acrylamide) nanohydrogel (ST/PL(AA-*cl*-AAm*)* NHG) by co-polymerization method which was used as an effective adsorbent for the removal of coomassie brilliant (CB) blue R-250 dye from the aqueous solution. The synthesized nanohydrogel was characterized by FTIR, SEM and TEM techniques. The effect of initial dye concentration, temperature, and agitation time on the adsorption ability of the nanohydrogel was studied comprehensively. The experimental outcomes exhibited that the prepared nanohydrogel had high adsorption tendency to remove the CB from the aqueous solution. The regression coefficient values for Langmuir (0.99), Frendluich (0.93) and Tempkin (0.98) recommended that adsorption process fit to langmuir isotherm. The pseudo-second-order equation showed the better adsorption kinetics of the adsorption process. The feasibility of CB adsorption onto ST/PL(AA-*cl*-AAm*)* NHG was also studied thermodynamically and the results indicated that the adsorption was spontaneous and chemical in nature.

Keywords: Starch/poly(alginic acid-*cl*-acrylamide); Nanohydrogel; Coomassie brilliant blue; Adsorption

1. Introduction

Due to the fast industrialization, the addition of various types of pollutants to the water system is one of the common problems worldwide. Addition of harmful metal ions, industrial dye molecules, phenols, fertilizers pollute the natural water bodies, which makes it unfavorable for the use by animals as well as by plants (Rivaz & Munoz, 2010; Rao, Mohapatra, Anand & Venkateswarlu, 2010; Kyzas & Lazaridis, 2009; Sharma et al., 2015; Santhi, Manonmani, Vasantha& Chang, 2011; Kumar et al., 2016). Due to the toxic nature of water, it can cause numerous problems such as jaundice, high heart beat rate, vomiting and skin problems. The presence of dyes and metal ions in the water can be carcinogenic to animals and humans (Sharma et al., 2017; Kumar et al., 2017). Various techniques have been applied for the removal of these pollutants from aqueous medium (Pathania, Sharma & Thakur, 2015; Naushad et al, 2016a, 2016b, 2016c). Adsorption is one of the best solutions for the removal of dyes from the wastewater due to its cost-effective nature (Alqadami et al. 2016; Bahram et al. 2011). Adsorption by the super adsorbing materials such as nano- sized hydrogels has made this field more important (Zhang, Zhou, Zhou & Shuang, 2012; Meng, Wang, Xu & Li, 2012; Patel & Patel, 2013; Kasgoz, Durmus & Kasgoz, 2008; Sun, Wang & Duo, 2012). Due to the small size and three-dimensional structures, nanohydrogels can be used in a number of applications such as drug delivery, water purification, adsorption, electrode making, or as smart materials. Their absorbing tendency can be easily tuned by adjusting the pore size and their chemical structure (Yang et al., 2013; Balkrishnan& Banerjee, 2011; Vlierberghe, Dubruel & Schacht, 2011). Hydrogels are flexible in nature and have the capacity to retain water due to functional groups attached to the polymeric backbone. By changing the nature and chemistry of the precursor

hydrogel, their mechanical properties can be improved efficiently (Anbia & Ghaffari, 2009; Hameed &Ahmad, 2009; Langmuir, 1916). Hydrogels can be categorized based on chemical and physical nature of crosslinked junctions. Different approaches have been used for designing of nanohydrogels, out of which first approach includes the physical attraction between the polymeric chains. Yu et al. has synthesized chitosan-based nanohydrogels via physical (electrostatic) attractions only. In contrast, the second approach includes the formation of nanohydrogels by chemical methods. For example, Bronich *et al.* synthesized a copolymer nanohydrogels by chemically crosslinking the constituting polymers (Strandman & Zhu, 2016, Phadke et al., 2012; Akay et al., 2013; Krogsgaard, Behrens, Pedersen & Birkedal, 2013; Wei et al.,2014, Appel et al., 2012; Chirila et al., 2014). The third approach includes different polymerization techniques such as mini polymerization, reverse polymerization or precipitation polymerization.

Starch is a natural polymer and having various applications. It has substituted many conventionally used non-renewable materials and has occurred as an excellent base for the support of different compounds. Due to its inexpensive and biodegradable nature, it seems to be more favorable. The performance of starch can be effectively improved by the co-grafting and cross-linking approach (Puppi, Chiellini, Piras & Chiellini, 2010; Gomes et al., 2002; Neves, Kouyumdzhiev& Reis, 2005; Schieker et al., 2006; Mano et al., 2004; Elvira, Mano, Roman & Reis, 2002; Reis & Cunha,1995). This resulted in better mechanical properties and water stability of starch. It is also used in industry at a large scale as wrap sizing, since it increases the strength to a greater extent.

In the present paper, we have synthesized starch/poly(alginic acid-*cl*-acrylamide) nanohydrogel which was efficaciously used for the removal of coomassie brilliant blue R-250

dye from aqueous medium due to its high adsorbing ability. The equilibrium removal efficiency was studied using Langmuir, Freundlich and Tempkin isotherm models.

2. Experimental protocol

2.1. Reagents and instruments

The main reagents were alginic acid (LobaChemie), acryl amide (LobaChemie), starch (LobaChemie), ammonium persulphate (CDH Pvt. Ltd., India), N,N–methylene bis-acryl amide (S-D fine chem. Ltd.).Various instruments used were shaker (INCO Instrument and Chemical Private Limited), centrifuge machine (INCO Instrument and Chemical Private Limited.), double beam UV spectrophotometer (INCO Instrument and Chemical Private Limited), FTIR (Agilent technologies Cary 630 FTIR), Scanning electron microscopy (JEOL. Model, JSM 610), Transmission electron microscopy (Techni G2 20 S-Twin).

2.2. Synthesis of starch/poly(alginic acid-*cl*-acrylamide) nanohydrogel

The ST/PL(AA-*cl*-AAm)NHG was prepared by co-graft polymerization method. The solution of starch (5%) was prepared in double distilled water with constant stirring using magnetic stirrer. To the above prepared starch gel, 0.1M alginic acid (AA) and 0.1M acrylamide (AAm) solutions were added drop wise in the presence of initiator, APS (5%) and cross linker, *N*,*N'*-Methylenebisacrylamide (MBAAm) (7%). The reaction mixture was vigorously stirred for 4 h at 65°C using thermostat. The ST/PL(AA-*cl*-AAm)NHG was collected after 4 h using acetone and dried at 50°C in hot air oven. The reaction yield was calculated using formula:

$$\%\, yield = \frac{W_R - W_P}{W_R} X100, \qquad (1)$$

2.3. Characterization

FTIR spectra for ST/PL(AA-*cl*-AAm)NHG and dye adsorbed ST/PL(AA-*cl*-AAm)NHG was recorded by Fourier-transform infrared spectrophotometer using KBr disk method. The FTIR spectrum was recorded in the wave number range from 400 to 4000 cm^{-1}. Microphotographs of nanohydrogels were recorded by using scanning electron microscope (SEM). The two samples were placed on a carbon tape with silicon adhesive and mounted on an aluminum stub. The microphotographs were obtained at different magnifications. The particle size of ST/PL(AA-*cl*-AAm)NHG was carried out using transmission electron microscope (FEI 200 kV, Technai). The particle dimension and morphology were determined by preparing the suspensions of prepared nanohydrogel in ethanol and positioned on carbon copper grid.

2.4. Adsorption of hazardous coomasie brilliant blue R-250 (CB)

Adsorption of toxic coomasie brilliant blue R-250 **(**CB) dye (scheme 1) from aqueous phase was studied by batch technique. 50 mL of CB solution with varying initial dye concentrations was shaken with a known amount of adsorbent in 100 mL Erlenmeyer flask at 30°C. The experimental flasks were taken out at fixed time interval until the adsorption equilibrium was achieved. The dye solution was separated by centrifugation operated at 3500 rpm for 5 min. The supernatants were then filtered to ensure that solutions were free from ST/PL(AA-*cl*-AAm)NHG before measuring the residual CB concentration. The remaining dye in the filtrate was analyzed by UV-visible spectrophotometer (Shimadzu UV-1601) at 555 nm. The effect of agitation time, initial CB dye concentration, adsorbent amount, pH and temperature were studied and optimized for the maximum adsorption of dye. The experiments were conducted in the duplicate and

negative controls were simultaneously carried out. The % removal and amount of dye adsorption per unit mass of ST/PL(AA-*cl*-AAm)NHG at equilibrium were evaluated as:

$$qe = \frac{(Co - Ce)V}{m} \qquad (2)$$

$$\% \text{ Adsorption} = \frac{C_0 - C_e}{C_0} \times 100 \qquad (3)$$

3. Results and discussion

3.1. Synthesis and characterization

The ST/PL(AA-*cl*-AAm)NHG was synthesized using co-graft polymerization method in the presence of initiator APS and crosslinker *N,N'*-methylene bis-acrylamide. The reaction yield of the prepared nanohydrogel was found to be 85%. The detailed synthesis of the nanohydrogel is shown in the scheme-2.

3.2. Characterization

Fig. 1 shows the FTIR spectrum of ST/PL(AA-*cl*-AAm)NHG; before and after CB dye adsorption. The peaks at 1114 cm^{-1}, 1589 cm^{-1} and 3390 cm^{-1} were assigned to the C–O stretching, C=O stretching and O–H stretching vibrations, respectively for the starch moiety (Sharma, Pathania & Naushad, 2016). The characteristic peak at 3433 cm^{-1} was observed for -OH stretching (Miller & Wilkins, 1952; Sharma et al., 2016). Fig. 2a,b shows the SEM images of ST/PL(AA-*cl*-AAm)NHG at different magnifications which showed the smooth and fibrous surface of the nanohydrogel. Fig. 2c,d shows the TEM images of prepared nanohydrogel at different magnifications. These images indicated the appearance of smooth surface with average size of particles ranging from 30-80 nm on the surface of the nanohydrogel.

3.3. Sequestration and optimization of CB dye from aqueous phase

3.3.1. Effect of initial dye concentration

The effect of initial CB concentration was carried out by varying the dye concentration from 20 to 120 mg/L. It is clear from Fig. 3(a) that the percentage dye uptake decreased progressively with increasing initial dye concentration upto 120 mg/L. The higher percentage of dye removal at low concentration could be ascribed to the low ratio of initial number of dye molecules on the surface site of hydrogel. However, at relatively higher concentrations, the removal percentage was decreased due to the availability of lesser sorption sites. The active surface sites are important for the adsorption of dye molecules which are absent at higher concentration (Fu & Wang, 2011; Naushad et al., 2016d).

3.3.2. Effect of adsorbent amount

Fig. 3b indicates that increase in adsorbent loading boost the % uptake of CB which was due to availability of greater active sites as well as optimal surface area containing copious pores with available volume supplying more functional groups boosting the adsorption of dye (CB) molecules. However, after 0.1g /50 mL of adsorbent loading, no significant percentage uptake was observed. Actually, adsorbent particles grouped together to form cluster, so there was no significant increase in specific surface area of ST/PL(AA-*cl*-AAm)NHG (Barka et al., 2011). Although the % efficiency increased with adsorbent amount, but the amount of dye (CB) adsorbed per unit mass (q_e) diminished as shown in Fig. 3(b). It was ascribed to the unsaturation of active surface sites on adsorbent (ST/PL(AA-*cl*-AAm)NHG) due to increase in the ratio of adsorption sites to the dye molecules (Ozacar & Sengil, 2005).

3.3.3. Effect of pH of adsorbate solution

In order to examine the pH sensitivity of the prepared nanohydrogel, the effect of pH on the dye (CB) solution is illustrated in Fig. 3(c). During the sorption of CB from aqueous system, diverse interactions occurred between hydrogel and CB dyes such as ion-exchange, hydrophobic attractions, chemical bonding, hydrogen bonds, van-der Waals force, physical adsorption, dye-dye interactions etc. (Crini & Badot, 2008). The maximum removal of anionic CB dye was observed during the pH range of 2.0 to 5.0 and then % efficiency declined sharply from 78.56 to 28.78%. At lower pH (2.0-5.0), fraction of functional groups accommodated on the surface of hydrogel gets protonated and acquires positive charge. Thus, the electrostatic interaction occurred between hydrogel and anionic CB dye. However, at higher pH, the concentration of hydrogen ion became lower and competition of H^+ ion with the anionic dye molecules becomes negligible. Therefore, the interaction between adsorbent and CB dye decreased, leading to the minimum sorption rate. Consequently, the pH (5.0) was preferred for subsequent experiments.

3.3.4. Effect of agitation time

The effect of agitation time for the remediation of noxious dye by adsorbent was investigated in the range of 30 to 180 min at room temperature (Fig. 3d). The adsorption percentage was increased with increasing the contact time and reached plateau after 150 min. At the starting, more vacant surface sites were available for the adsorption of CB during and with the passage of time; the remaining vacant sites were difficult to be occupied due to repulsive forces between the solute molecules onto adsorbent and liquid phase. Thus, for all subsequent equilibrium adsorption studies, contact time was optimized at 150 min.

3.3.5. Effect of temperature

Fig. 4 reveals the effect of temperature on sorption under the optimized conditions of dye concentration, sorbent amount, agitation time and pH of sorbate solution. It has been observed as temperature increases from 30°C to 55 °C the adsorption of CB also increase, it is because as the temperature rises it leads to more activation of ST/PL(AA-*cl*-AAm)NHG surface. The enhancement of adsorption capacity with temperature is synergistic with raising the diffusion rate of adsorbate molecules with adequate energy to undergo the interaction with active surface sites of hydrogel or enlargement of internal structure of adsorbent particles. The outcomes also specify that the sorption of CB dye onto hydrogel is an endothermic process.

3.3.6. Equilibrium study

In order to determine the adsorption capacity of ST/PL(AA-*cl*-AAm)NHG, the experimental data are well fitted to the Langmuir, Freundlich and Tempkin isotherm models (Tofighy & Mohammadi, 2011).

3.3.6.1. Langmuir Isotherm

The linearized form of Langmuir model (Langmuir 1916) can be represented as follows:

$$\frac{C_e}{q_e} = \frac{1}{K_L Q_m} + \frac{C_e}{Q_m} \qquad (4)$$

The linear regression between C_e/q_e vs. C_e allows the computation of R^2 value, which conforms to be 0.99, referring the monolayer adsorption of CB (Fig. 5a). Significantly, the maximum adsorption capacity (Q_m) obtained from the slope of linear plot was 31.24 mg g^{-1} (Table 1).

Another parameter in the Langmuir isotherm, a dimension less separation factor (R_L), which is defined as follows:

$$R_L = \frac{1}{1+K_L C_0} \qquad (5)$$

The calculated values of R_L were found to be favorable during the whole range of dye concentration (0.47-0.12) (Foo, 2012).

3.3.6.2. Freundlich isotherm

The linearized form of this model can be given as below (Freundlich 1906):

$$\log q_e = \log k_F + \frac{1}{n}\log C_e \qquad (6)$$

A plot of log q_e vs. log C_e allows the constant and exponent n to be computed from the slope and intercept, respectively. The Freundlich adsorption constants are shown in Table 1. The low R^2 (0.93) obtained from this model suggested the inapplicability of Freundlich isotherm for the analysis of experimental data (Fig. 5b).

3.3.6.3. Tempkin model

This model is given as:

$$q_e = \frac{RT}{b}\ln(K_T C_e) \qquad (7)$$

Linearized Tempkin isotherm equation can be presented as follow (Ghasemi et al. 2014):

$$q_e = B_t\ln(K_T) + B_t\ln(C_e) \qquad (8)$$

The Tempkin parameters B_t and K_T were determined from a plot of q_e vs. lnC_e (Fig. 5c). It was revealed from Figure 5c that this model provides higher correlation coefficient (0.98) and discuss its suitability for the adsorption of CB onto ST/PL(AA-*cl*-AAm)NHG.

A comparison of maximum CB dye adsorption capacities of ST/PL(AA-*cl*-AAm)NHG with that of the other previously reported adsorbents is presented in Table 2. It was noted that ST/PL(AA-*cl*-AAm)NHG had better adsorption capacity compared to other adsorbents. So, ST/PL(AA-*cl*-AAm)NHG is a potential candidate for CB dye removal from aqueous medium.

3.4. Adsorption kinetics

Kinetic studies of sorption process present the significant information such as time required to attain the equilibrium, adsorption rate and prediction of adsorbate concentration in each phase after the equilibrium is reached (Febrianto et al., 2009). In the present work, reaction based model such as pseudo-first-order, pseudo-second-order kinetics were applied and mechanism of adsorption was exploited by plotting the experimental data with Weber-Morris model.

3.4.1. Pseudo-first-order equation

Lagergren revealed a method for adsorption analysis namely pseudo-first-order kinetic equation (Lagergren 1898; Ho 1998). The linear form of first-order kinetic equation is given as:

$$\ln(q_e - q_t) = \ln q_e - kt \qquad (9)$$

where k_1 (min^{-1}) is the rate constant for pseudo-first-order model (Savic & Vasic, 2006; Zhao, Li &Xiangke, 2011; Li et al., 2010). The value of k_1 and q_e were evaluated from the slope and intercept of $\ln(q_e-q_t)$ vs. t, respectively (Fig. 6a). The pseudo-first-order rate constants and regression coefficient are listed in Table 3.

3.4.2. Pseudo-second-order equation

It is presented in linear form as:

$$\frac{t}{q_e} = \frac{1}{k_2 q_e^2} + \frac{t}{q_e} \qquad (10)$$

where k_2 is the overall rate constant for pseudo-second-order kinetics (g $mg^{-1}min^{-1}$). A plot of t/q_t against t gives a linear relationship, from which the value of q_e and k_2 can be evaluated from the slope and intercept, respectively (Reddy, Kannamba & Rao, 2010). The plot of pseudo-second-order kinetics onto ST/PL(AA-*cl*-AAm)NHG is given in Fig. 6(b). The values of k_2, q_e and

regression coefficient (R^2) are given in Table 3. So according to, Fig. 6b and Table 3, the experimental data fit very well for CB adsorption with stronger correlation coefficient (0.98).

3.5. Adsorption mechanism

3.5.1. Weber-Morris model

The Weber-Morris model (Weber and Morris 1962) was designed to identify the diffusion mechanism of adsorbate molecules involved in the sorption process. This model assumes an empirically based functional relationship commonly recommended for adsorption, where the uptake of dye solution varies almost proportionally to $t^{0.5}$ instead of contact time (t).

$$q_t = K_{dif}\, t^{0.5} + C \qquad (11)$$

where k_{dif} (mg/(g $min^{0.5}$)) is the intra-particle diffusion rate constant and C (mg/g) is the intercept, which indicates the thickness of the boundary layer and larger value of C reflects the greater boundary layer effect. The fitting plot of q_t against $t^{0.5}$ is shown in Fig. 6c. If the intra-particle diffusion occurs, plot passes through the origin, then intra-particle diffusion is the only the rate limiting step. As inferred from Fig. 6c, plot for intra-particle diffusion appears to display the multiple straight lines, which exhibit the participation of multistage adsorption. The intra-particle diffusion curve appears to be divided into the three distinctive linear regions. The first phase obtained during initial time period indicates the external mass transfer which involve transportation of CB dye from liquid phase to the solid boundary of ST/PL(AA-*cl*-AAm)NHG, the second curve ascribed to film diffusion and third region at higher contact time, exhibits gradual adsorption stage which is dominated by pore diffusion (Pan et al., 2012; Islam, Mishra & Patel, 2010; Gupta & Bhattacharyya, 2011).On the basis of these results, it became quite clear that adsorption of CB dye from aqueous phase was not completed in one step instead it is a

multifaceted process in which some other mechanism along with intra-particle diffusion edicts the sorption process.

3.6. Thermodynamic properties

The adsorption process depends on temperature and coupled with numerous thermodynamic parameters. Thermodynamic constants which include ΔG^0, ΔH^0 and ΔS^0 were computed by the following Eqn.

$$\Delta G^0 = -RT \ln k_0 \quad (12)$$

The equilibrium constant,

$$\ln k_0 = \frac{q_e}{C_e} \quad (13)$$

where q_e and C_e are the equilibrium concentration of CB onto ST/PL(AA-*cl*-AAm)NHG and in the solution, respectively. The distribution coefficient can be expressed in terms of enthalpy and entropy changes as a function of temperature:

$$\ln K_0 = \frac{\Delta S^\circ}{R} - \frac{\Delta H^\circ}{RT} \quad (14)$$

The values of ΔH^0 and ΔS^0 were found from the slope and intercept of a plot ln K_0 vs. 1/T (Fig. 7). The positive value of ΔH^0 (17.15 kJ mol^{-1}) affords the endothermic nature of adsorption process because adsorbate species (CB) have to shift the more than one water molecule and resulted in endothermic adsorption process. The positive value of ΔS^0 (60.64 J mol^{-1} K^{-1}) indicates that randomness increased at solid-liquid interface with the structural changes in the adsorbate and adsorbent molecules. It also contributes to enhancement in the degree of freedom during the adsorption of CB ions from aqueous solution. The water molecules, which were diffused or displaced by the adsorbate molecule, gain extra amount of transitional entropy and

permit the randomness in the system (Kyzas, Kostoglou & Lazaridis, 2009). The negative value of ΔG^0 (-1.25 kJ mol^{-1}) at 30 °C satisfy the feasibility and spontaneity of the adsorption process (Table 3).

Conclusions

In the present study, starch/poly(alginic acid-*cl*-acrylamide) nanohydrogel (ST/PL(AA-*cl*-AAm)NHG) was synthesized by co-polymerization method. This nanohydrogel was effectively used for the removal of coomassie brilliant (CB) blue R-250 dye from the aqueous medium. The adsorption was immensely dependent upon various parameters such as temperature, pH, adsorbent and adsorbate concentration and time. The adsorption of CB onto ST/PL(AA-*cl*-AAm)NHG followed pseudo-second-order kinetics and the equilibrium data fitted well with Langmuir isotherm revealing the physical and momolayer of adsorption process. Overall, this study revealed that ST/PL(AA-*cl*-AAm*)* NHG was a potential candidate for the removal of CB dye from aqueous medium.

Acknowledgement

The authors would like to extend their sincere appreciation to the Deanship of Scientific Research at King Saud University for funding this work through the Research Group NO. RG-1436-034.

References

Abd-El-Aziz, A., Abdelghani, A., El-Sadany, S., Overy, D. (2016) Antimicrobial and anticancer activities of organoiron melamine dendrimers capped with piperazine moieties. Eur. Polym. J., 82, 307–323.

Ahmed, K.B.A., Kalla, D., Uppuluri, K.B., Anbazhagan, V. (2014) Green synthesis of silver and gold nanoparticles employing levan, a biopolymer from acetobacter xylinum NCIM 2526, as a reducing agent and capping agent. Carbohydr. Polym., 112, 539–545.

Akay, G., Raeisi, A, H., Tuncaboylu, D, C., Orakdogen, N., Abdurrahmanoglu, S., Oppermann, W., &Okay, O., (2013). Self-healing hydrogels formed in catanionic surfactant solutions. Soft Matter 9, 2254–2261.

Alqadmi, A., Naushad, M., Ahamd, T., Abdalla, M.A., ALOthman, Z.A., AlShehri, S.M. (2016) Synthesis and characterization of Fe_3O_4@TSC nanocomposite: Highly efficient removal of toxic metal ions from aqueous medium. RSC Adv. 6, 22679-22689.

Anbia, M., &Ghaffari, A., (2009). Adsorption of phenolic compounds from aqueous solutions using carbon nanoporous adsorbent coated with polymer.Appl. Surf.Sci. 255, 9487–9492.

Ansari, F., Ghaedi, M., Taghdiri, M., Asfaram, A. (2016) Application of ZnO nanorods loaded on carbon for ultrasonic assisted dyes removal: experimental design and derivative spectrophotometry method. Ultrason. Sonochem., 33, 197–209

Appel, E, A., Loh, X, J., Jones, S, T., Biedermann, F., Dreiss, C. A., &Scherman, O, A., (2012). Ultra high water- content supramolecular hydrogels exhibiting multi stimuli responsiveness.J. Am. Chem. Soc. 134, 11767–11773.

Bahram, M., Keshvari, F., Najafi-Moghaddam, P. (2011) Development of cloud point extraction using pH-sensitive hydrogel for preconcentration and determination of malachite green. Talanta, 85, 891–896.

Balakrishnan, B., Banerjee, R., (2011). Biopolymer-based hydrogels for cartilage tissue-engineering. Chem. Rev., 111, 4453–4474.

Barka, N., Qouzal, S., Assabbane, A., Nounhan, A., &Ichou, Y, A., (2011).Removal of Reactive Yellow 84 from aqueous solutions by adsorption onto hydroxyapatite.J. Saudi Chem. Soc. 15, 263–267.

Bujnakova, Z., Balaz, M., Dutkova, E., Balaz, P., Kello, M., Mojzisova, G., Mojzis, J., Vilkova, M., Imrich, J., Psotka, M. (2017) Mechanochemical approach for the capping of mixed core CdS/ZnS nanocrystals: elimination of cadmium toxicity. J. Coll. Interf. Sci., 486, 97–111.

Chirila, T, V., Lee, H, H., Oddon, M., Nieuwenhuizen, M, M., Blakey, I., &Nicholson, T, M., (2014). Hydrogen- bonded supramolecular polymers as self-healing hydrogels: effect of a bulky adamantyl substituent in the ureido-pyrimidinonemonomer.J. Appl. Polym. Sci.131, 39932.

Crini, G., &Badot, P, M., (2008). Application of chitosan, a natural amino polysaccharide, for dye removal from aqueous solutions by adsorption processes using batch studies: A review of recent literature. Prog.Polym. Sci. 33, 399-447.

Elvira, C., Mano, J, F., Roman, J. S., Reis, R, L., (2002).Starch-based biodegradable hydrogels with potential biomedical applications as drug delivery systems, Biomaterials 23, 1955–1966.

Febrianto, J., Kosaish, N, A., Sunarso, J., Indraswati, N., &Ismadji, S., (2009). Equilibrium and kinetic studies in adsorption of heavy metals using biosorbent: A summary of recent studies. J. Hazardous Materials. 162, 616-645.

Foo, K, Y., (2012). Preparation, characterization and evaluation of adsorptive properties of orange peel based activated carbon via microwave induced K_2CO_3 activation. Bioresour. Technol. 104, 679–686.

Freundlich, H.M.F., (1906) Over the adsorption in solution, J. Phys. Chem. 57, 385-470.

Fu, F., &Wang, Q., (2011).Removal of heavy metal ions from wastewaters: A review.J.Enviorn. Manage. 92, 407-418.

Ghasemi, M., Naushad, M., Ghasemi, N., Khosravi-fard, Y. (2014) A novel agricultural waste based adsorbent for the removal of Pb(II) from aqueous solution: Kinetics, equilibrium and thermodynamic studies, J. Ind. Eng. Chem, 20, 454-461.

Gomes, M, E., Godinho, J, S., Tchalamov, D., Cunha, A, M., &Reis, R, L., (2002). Alternative tissue engineering scaffolds based on starch: processing methodologies, morphology, degradation and mechanical properties.Mater. Sci. Eng. C 20, 19–26.

Gupta, S, S., & Bhattacharyya, K, G., (2011). Kinetics of adsorption of metal ions on inorganic materials: A review.Adv. Coll. Interf. Sci. 162, 39–58.

Hameed, B, H., &Ahmad, A, A., (2009).Batch adsorption of methylene blue from aqueous solution by garlic peel, an agricultural waste biomass.J.Hazard.Mater.164, 870-875.

Ho, Y.S., McKay (1998) Sorption of dye from aqueous solution by peat, Sorption of dye from aqueous solution by peat. Chem. Eng. J. 70, 115–124.

Islam, M., Mishra, P, C., &Patel, R, K., (2010).Physicochemical characterization of hydroxyapatite and its application towards removal of nitrate from water. J. Environ. Manage. 91,1883–1891.

Kasgoz, H., Durmus, A., &Kasgoz, A., (2008). Enhanced swelling and adsorption properties of AAm-AMPSNa/clay hydrogel nanocomposites for heavy metal ion removal.Polym. Adv. Technol. 19, 213–220.

Krogsgaard, M., Behrens, M, A., Pedersen, J, S., &Birkedal, H., (2013). Self-healing mussel-inspired multi-pH-responsive hydrogels.Biomacromolecules 14, 297–301.

Kumar, A, Sharma, G., Chengsheng, G., Naushad, M., Pathania, D., Dhiman, P., Kalia, S., (2016) Magnetically recoverable ZrO_2/Fe_3O_4/Chitosan nanomaterials for enhanced sunlight driven photoreduction of carcinogenic Cr (VI) and dechlorination & mineralization of 4-chlorophenol from simulated waste water. RSC Adv. 13251–13263.

Kumar, A., Shalini, Sharma, G., Naushad, M., Kumar, A., Kalia, S., Guo, C., Mola G T., (2017) Facile hetero-assembly of superparamagnetic $Fe_3O_4/BiVO_4$ stacked on biochar for solar photo-degradation of methyl paraben and pesticide removal from soil, J. Photochem. Photobio. A: Chemistry 337 118–131.

Kyzas G, Z., Lazaridis, N, K., (2009). Reactive and basic dyes removal by sorption onto chitosan derivatives. J. Coll. Inter. Sci., 331, 32–39.

Kyzas, G, Z., Kostoglou, M., &Lazaridis, N, K., (2009). Copper and chromium(VI) removal by chitosan derivatives—Equilibrium and kinetic studies. Chem. Eng. J. 152, 440–448.

Lagergren, S. (1898) About the theory of so called adsorption of soluble substances, Kungliga Svenska Vetenskapsakademiens, Handlingar, Band, 24, 1–39.

Langmuir, I., (1916). The constitution and fundamental properties of solids and liquids.Part 1.Solids.J. Am. Chem. Soc. 38, 2221–2295.

Li, N., Liu, S, Q., Zheng, T., Wang, P., &Jiang, P, J., (2010). Adsorption isotherm, kinetic and mechanism studies of some substituted phenols on activated carbon fibers. Chemical Engineering Journal 157, 348-356.

Mano, J, F., Sousa, R, A., Boesel, L, F., Neves, N, M., &Reis, R, L., (2004).Bioinert, biodegradable and injectable polymeric matrix composites for hard tissue replacement: state of the art and recent developments.Compos. Sci. Technol. 64, 789–817.

Meng, Y., Wang, J, N., Xu, L., Li, A, M., (2012). Fast removal of Pb2+ from water using new chelating fiber modified with acylamino and amino groups. Chin. Chem. Lett. 23, 496–499.

Miller, F, A., &Wilkins, C, H., (1952). Infrared spectra and characteristic frequencies of inorganic ions, Anal Chem 24, 1253–1294.

Naushad, M, Ahamad, T., Sharma, G, Al-Muhtaseb, AH, Albadarin, AB, Alam, MM, ALOthman, ZA, Alshehri, SM, Ghfar, AA, (2016a) Synthesis and characterization of a new starch/SnO2 nanocomposite for efficient adsorption of toxic Hg^{2+} metal ion. Chem. Eng. J., 300, 306-316.

Naushad, M., ALOthman, Z.A., Sharma, G., Inamuddin, (2016b). Kinetics, isotherm and thermodynamic investigations for the adsorption of Co(II) ion onto crystal violet modified amberlite IR-120 resin. Ionics 21, 1453-1459.

Naushad, M., Khan, M.R., ALOthman, Z.A., Awual, M.R., Alqadami, A. A. (2016c) Water purification using cost effective material prepared from agricultural waste: Kinetics, isotherms and thermodynamic studies. CLEAN–Soil, Air, Water 44, 1036-1045.

Naushad, M., Vasudevan, S., Sharma, G., Kumar, ALOthman, Z.A., (2016d) Adsorption kinetics, isotherms and thermodynamic studies for Hg^{2+} adsorption from aqueous medium using alizarin red-S loaded amberlite IRA-400 resin, Desal. Water Treat., 57 18551-18559.

Neves, N, M., Kouyumdzhiev, A., &Reis, R, L., (2005). The morphology, mechanical properties and ageing behavior of porous injection molded starch-based blends for tissue engineering scaffolding.Mater. Sci. Eng. C 25,195–200.

Ozacar, M., Sengil, I, A., (2005). Adsorption of metal complex dyes from aqueous solutions by pine sawdust.Bioresour. Technol. 96, 791-795.

Pan, Y, J., Chen, Y, Y., Wang, D, R., Wei, C., Guo, J., Lu, D, R., Chu, C, C., & Wang, C, C., (2012). Redox/pH dual stimuli-responsive biodegradable nanohydrogels with varying responses to dithiothreitol and glutathione for controlled drug release.Biomaterials 33, 6570-6579.

Patel Y, N., &Patel, M, P., (2013). A new fast swelling poly[DAPB-co-DMAAm-co-AASS] superabsorbent hydrogel for removal of anionic dyes from water.Chin. Chem. Lett. 24,1005–1007.

Pathania, D., Sharma, G., Thakur, R., (2015). Pectin @ zirconium (IV) silicophosphate nanocomposite ion exchanger: Photo catalysis, heavy metal separation and antibacterial activity. Chem. Eng. J. 267, 235-244.

Phadke, A., Zhang, C., Arman, B., Hsu, C, C., Mashelkar, R, A., Lele, A, K., &Varghese, S., (2012).Rapid self-healing hydrogels.PNAS 109 (2012) 4383–4388.

Puppi, D., Chiellini, F., Piras, A, M., Chiellini, E., (2010).Polymeric materials for bone and cartilage repair.Prog.Polym. Sci. 35, 403–440.

Rao, K, S., Mohapatra, M., Anand, S., Venkateswarlu P.,(2010). Review on cadmium removal from aqueous solutions.Int. J. Eng. Sci. Technol. 2, 81–103.

Reddy, L.K., Kannamba, B., Rao, V.B.A. (2010) Removal of Cu(II) from aqueous solutions using chemically modified chitosan, J. Hazard. Mat. 175, 939-948.

Reis, R, L., Cunha, M., (1995).Characterization of two biodegradable polymers of potential application within the biomaterials field. Mater. Sci. 6, 786–792.

Rivas, B, L., & Munoz, C.,(2010). Functional water-insoluble polymers with ability to remove arsenic (V).Polym. Bull.65, 1–11.

Sales, P.F.D., Magriotis, Z.M., Rossi, M.A.L.S., Resende, R.F., Nunes, C.A. (2013) Optimization by Response Surface Methodology of the adsorption of Coomassie Blue dye on natural and acid-treated clays. J. Environ. Manag.,130, 417–428.

Santhi T., Manonmani, S.,Vasantha V, S., Chang, Y, T., (2016). A new alternative adsorbent for the removal of cationic dyes from aqueous solution. Arab. J. Chem. 9, 466-474.

Savic, J, Z., &Vasic, V, M., (2006). Thermodynamics and kinetics of 1,8-dihydroxy-2-(imidazol-5-ylazo)-naphthalene-3,6-disulphonic acid immobilization on Dowex resin 278, 197-203.

Schieker, M., Seitz, H., Drosse, I., Seitz, S., &Mutschler, W., (2006). Biomaterials as scaffold for bone tissue engineering. Eur. J. Trauma 32, 114–124.

Sharma, G, Naushad, M., Al-Muhtaseb, A.H., Kumar, A., Khan, M R., Kalia, S., Shweta, Bala, M., Sharma, A., (2017) Fabrication and characterization of chitosan-crosslinked-poly(alginic acid) nanohydrogel for adsorptive removal of Cr(VI) metal ion from aqueous medium, Intern. J. Biolog. Macrom. 95 484-493.

Sharma, G., Kumar, A., Naushad, M., Pathania, D., &Sillanpa, M., (2016).Polyacrylamide@Zr(IV) vanadophosphate nanocomposite: Ion exchange properties, antibacterial activity, and photocatalytic behavior. J. Ind. Eng. Chem., 33, 201-208.

Sharma, G., Naushad, M., Kumar, A., Devi, S., Khan, M.R., (2015). Lanthanum/Cadmium/Polyaniline bimetallic nanocomposite for the photodegradation of organic pollutant. Iran. Polym. J., 24 1003-1013.

Sharma, G., Pathania, D., Naushad, M., (2014).Fabrication, characterization and antimicrobial activity of polyaniline Th (IV) tungstomolybdophosphate nanocomposite material: Efficient removal of toxic metal ions from water, Chem. Eng. J., 251, 413-421.

Strandman, S., &Zhu, X, X., (2016). Self-healing supramolecular hydrogels based on reversible physical interactions. Gels 1–31.

Sun, J, X., Wang, Y, L., &Dou, S, H., (2012). A novel positively thermo-sensitive hydrogel based on ethylene diamine tetraaceticdianhydride and piperazine: design, synthesis and characterization. Chin. Chem. Lett.23, 97–100.

Tofighy, A, M., &Mohammadi, T., (2011).Adsorption of divalent heavy metal ions from water using carbon nanotube sheets. J. Hazard. Mat., 185, 140-147.

Vlierberghe, S, V., Dubruel, P., &Schacht, E., (2011). Biopolymer-based hydrogels as scaffolds for tissue engineering applications: a review. Biomacromol., 12 1387–1408.

Weber, W.J., Morris, J.C. (1962) Advances in water pollution research: removal of biologically resistant pollutant from wastewater by adsorption. In Proceedings of the Intern. Conf. on Water Pollution Symposium, vol. 2, pp. 231–266, Pergamon Press, Oxford, UK.

Wei, Z., Yang, J, H., Zhou, J., Xu, F., Zrínyi, M., Dussault, P. H., &Chen, Y.N., (2014). Self-healing gels based on constitutional dynamic chemistry and their potential applications. Chem. Soc. Rev. 43, 8114–8131.

Yang, J., Han, C, R., Duan, J, F., Xu, F., &Sun, R, C., (2013). Mechanical and viscoelastic properties of cellulose nanocrystals reinforced poly(ethylene glycol) nanocomposite hydrogels. ACS Applied Mat. Interf.. 5, 3199–3207.

Zhang M, C., Zhou, Q., Zhou, Y., Shuang, C, D., (2012). Efficient adsorption and desorption of Cu^{2+} by a novel acid-resistant magnetic weak acid resin. Chin. Chem. Lett.23, 1267–1270.

Zhao, G., Li, J., &Xiangke, W., (2011).Kinetic and thermodynamic study of 1-naphthol adsorption from aqueous solution to sulfonated graphene nanosheets. Chem. Eng. J., 173,185-190.

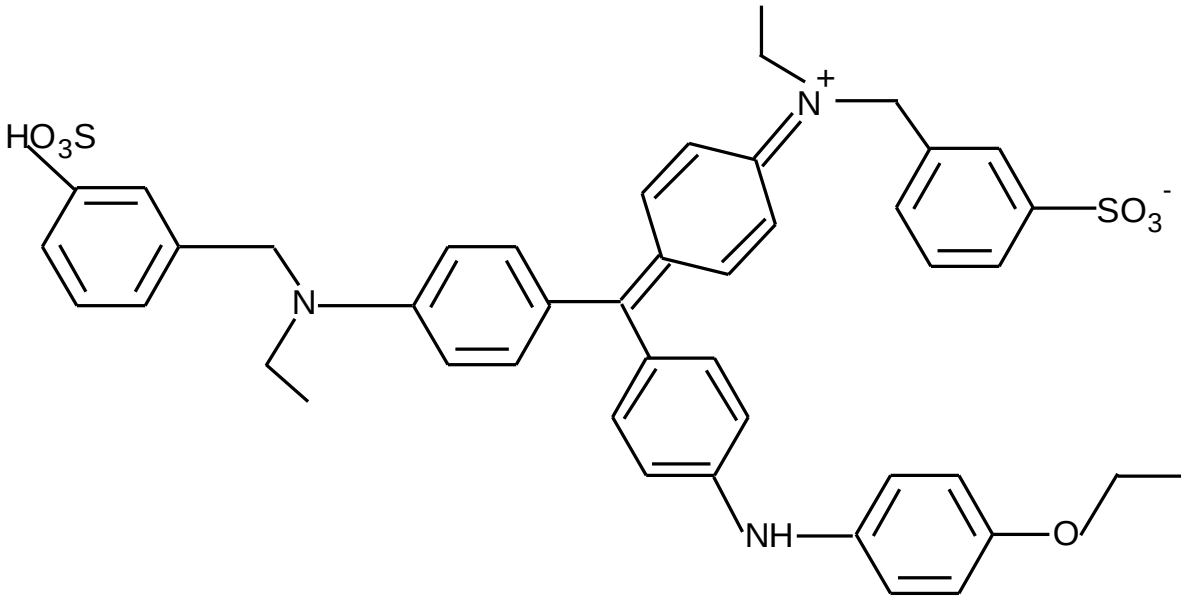

Scheme-1. Structure of coomasie brilliant (CB) blue R-250 dye

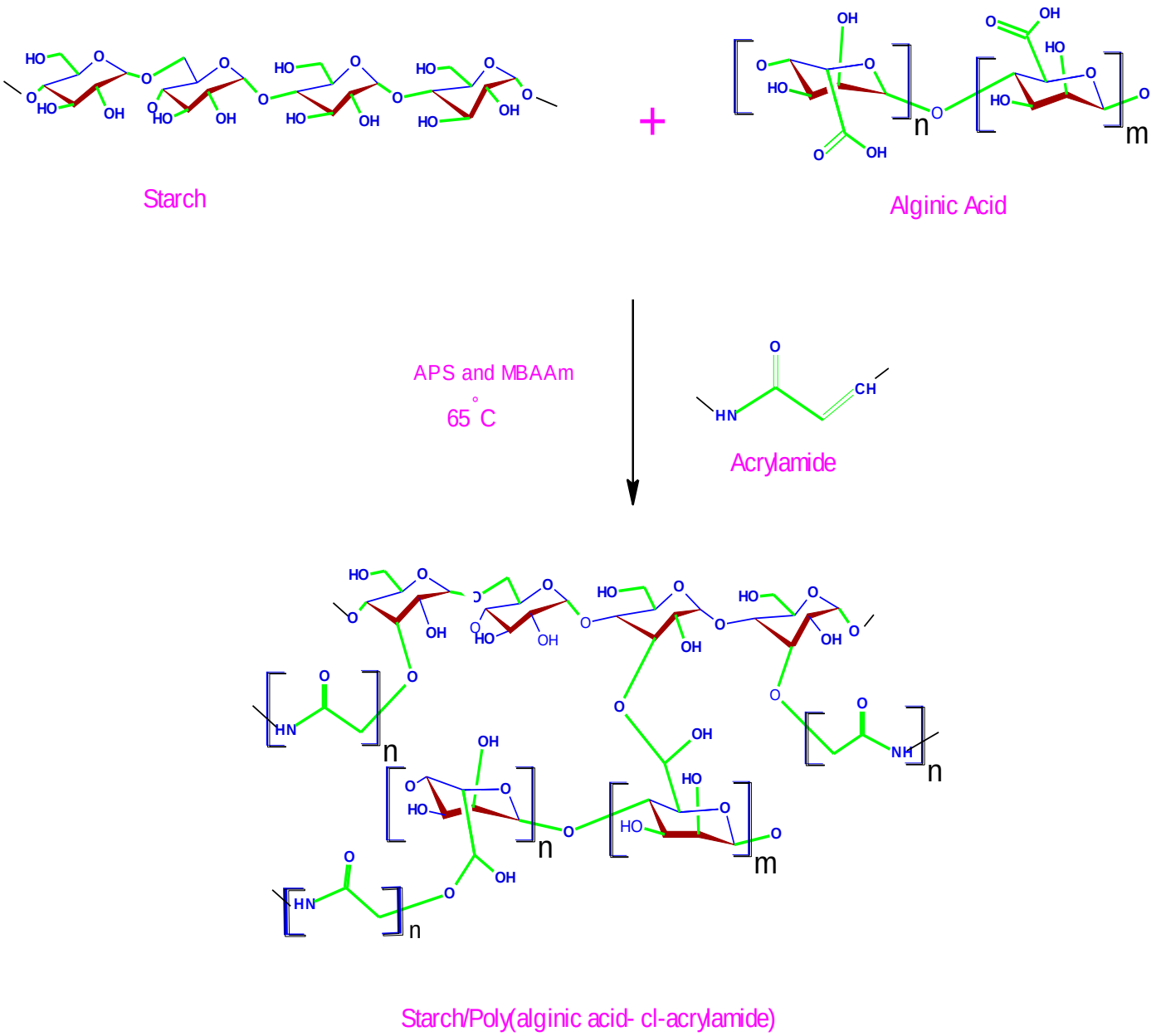

Scheme 2. Synthesis of ST/PL(AA-*cl*-AAm) NHG

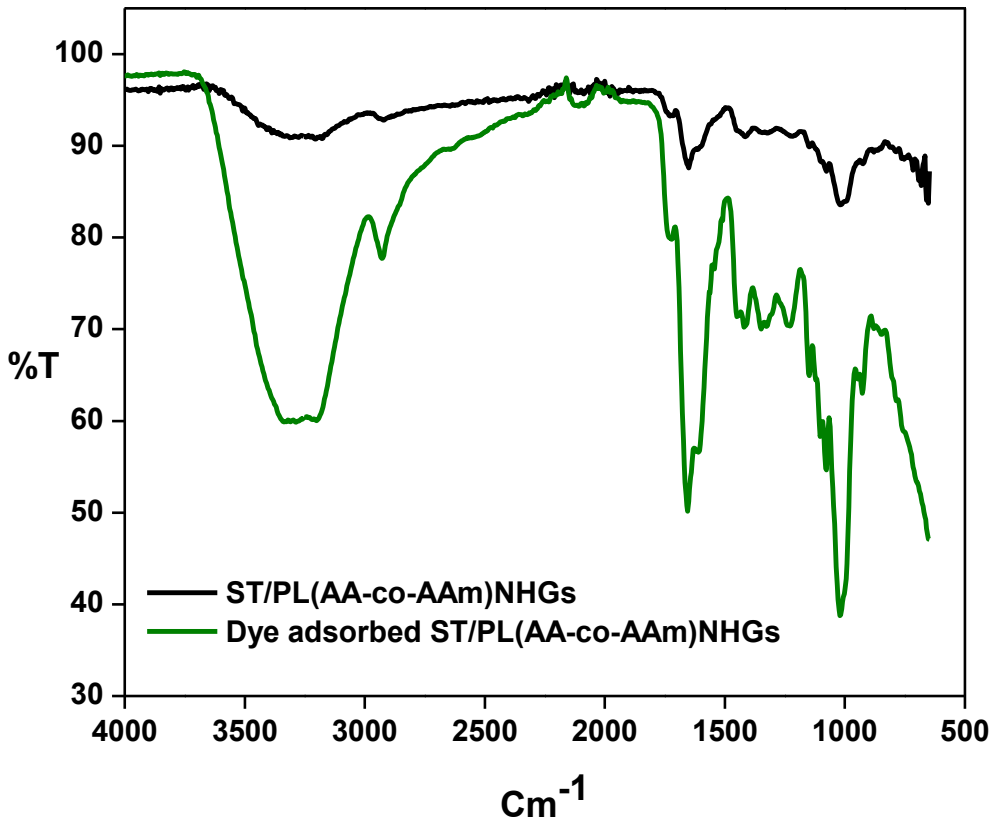

Fig. 1 FTIR spectra of ST/PL(AA-*cl*-AAm*)* NHG before and after CB dye adsorption

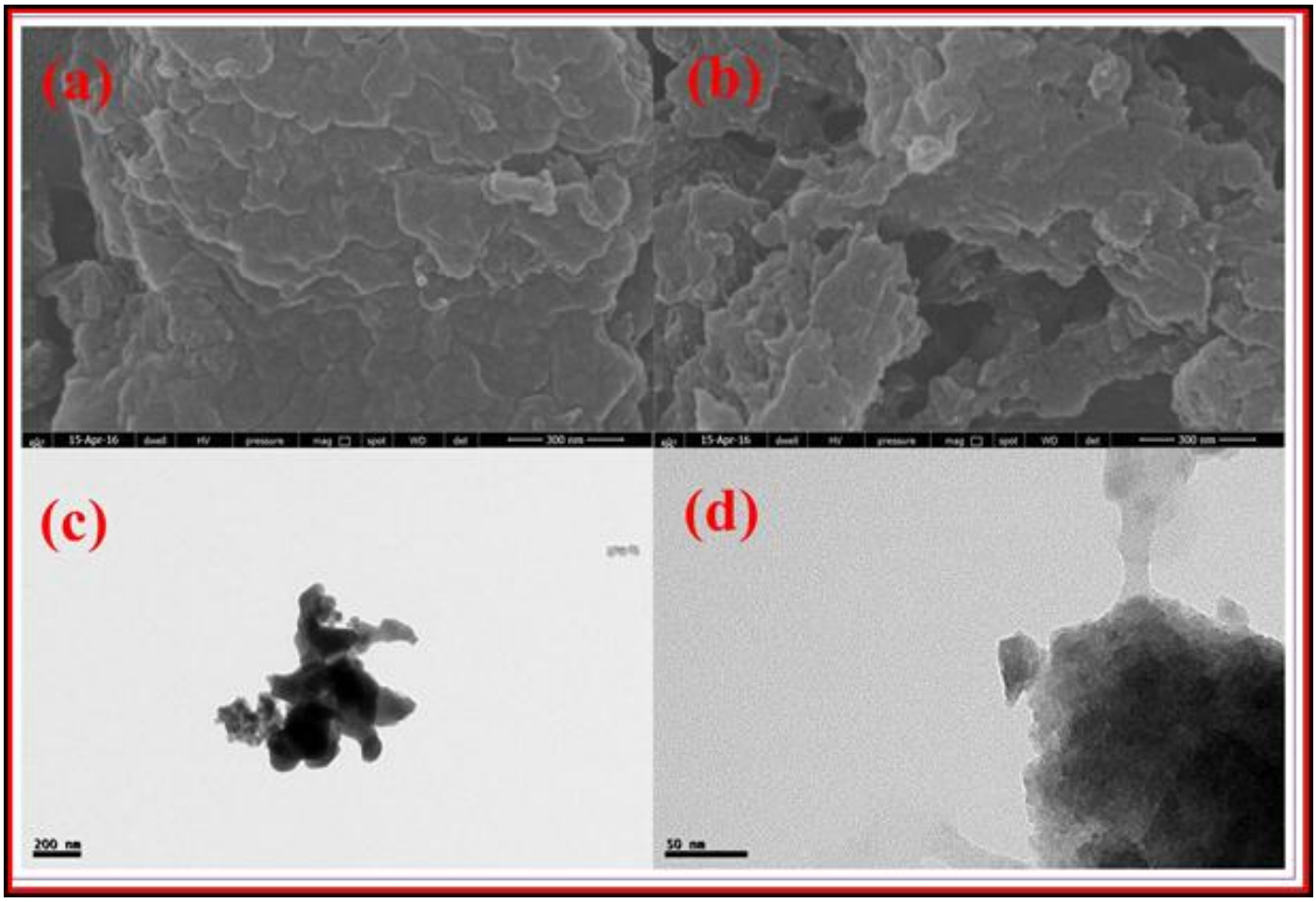

Fig. 2 SEM images of ST/PL(AA-*cl*-AAm*)* NHG (a) before adsorption and (b) after adsorption of CB dye; TEM images of ST/PL(AA-*cl*-AAm*)* NHG (c) before adsorption and (d) after adsorption of CB dye

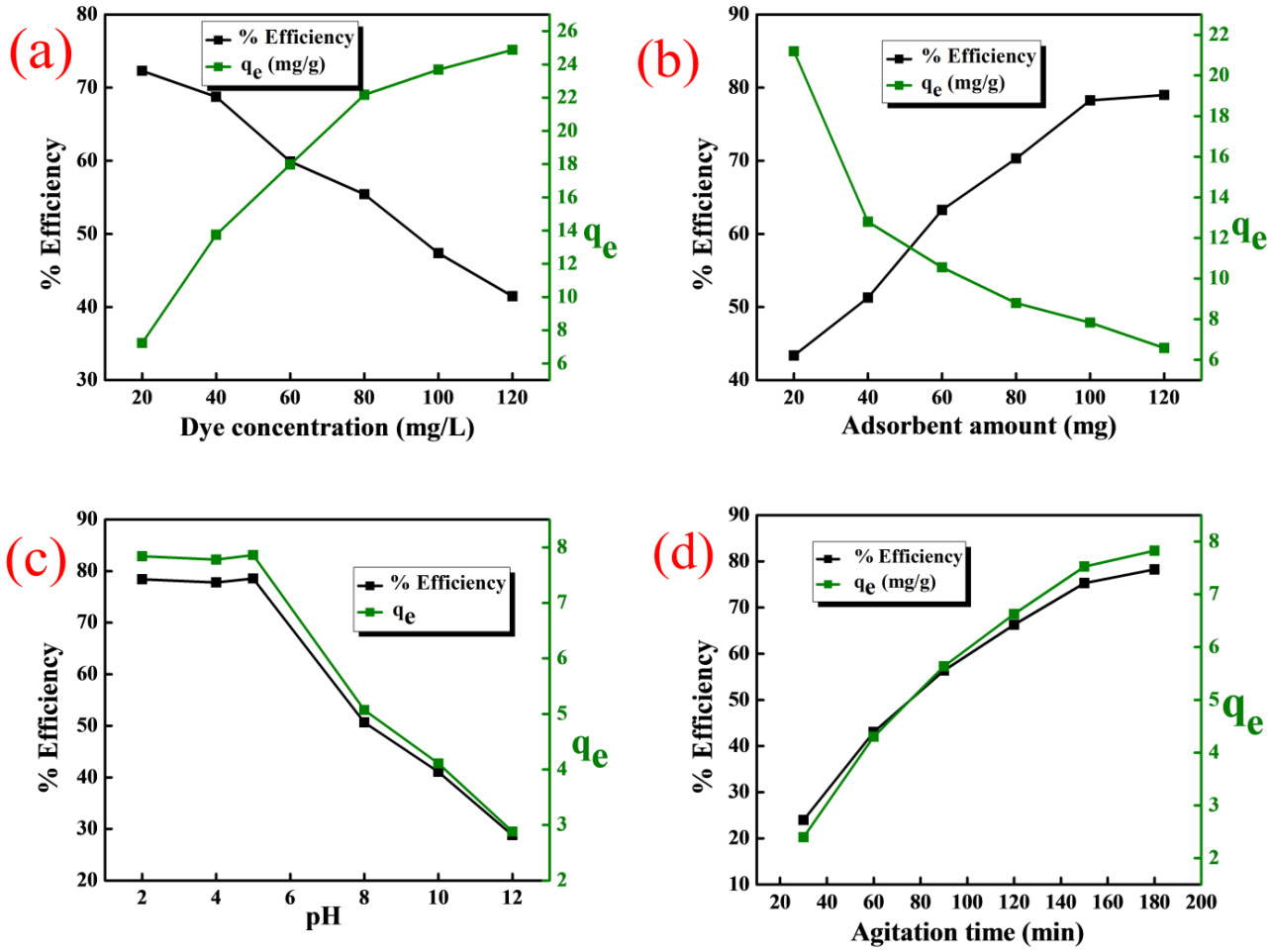

Fig. 3. Effect of (a) initial dye concentration (b) adsorbent amount (c) pH (d) agitation time on the adsorption of CB dye onto ST/PL(AA-*cl*-AAm) NHG

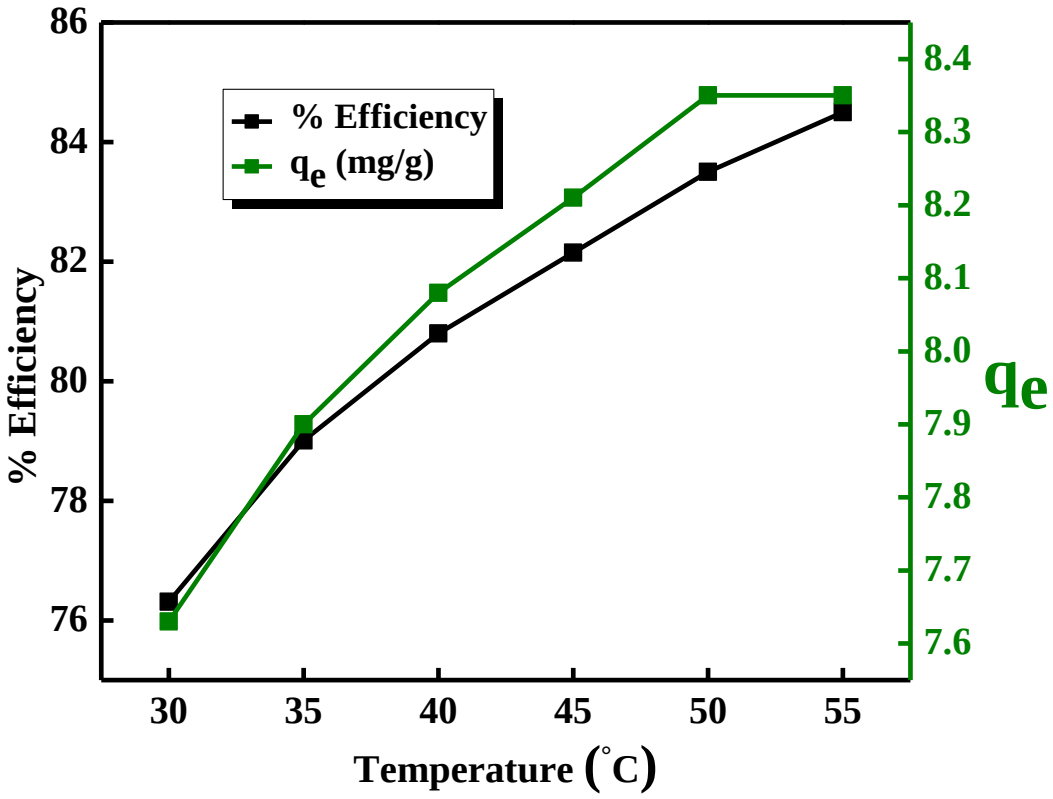

Fig.4. Effect of temperature on the removal of CB at 0.1 g of ST/PL(AA-*cl*-AAm*)* NHG in 50 mL at pH 5.0, dye concentration 20 mg L^{-1} and agitation time 150 (min)

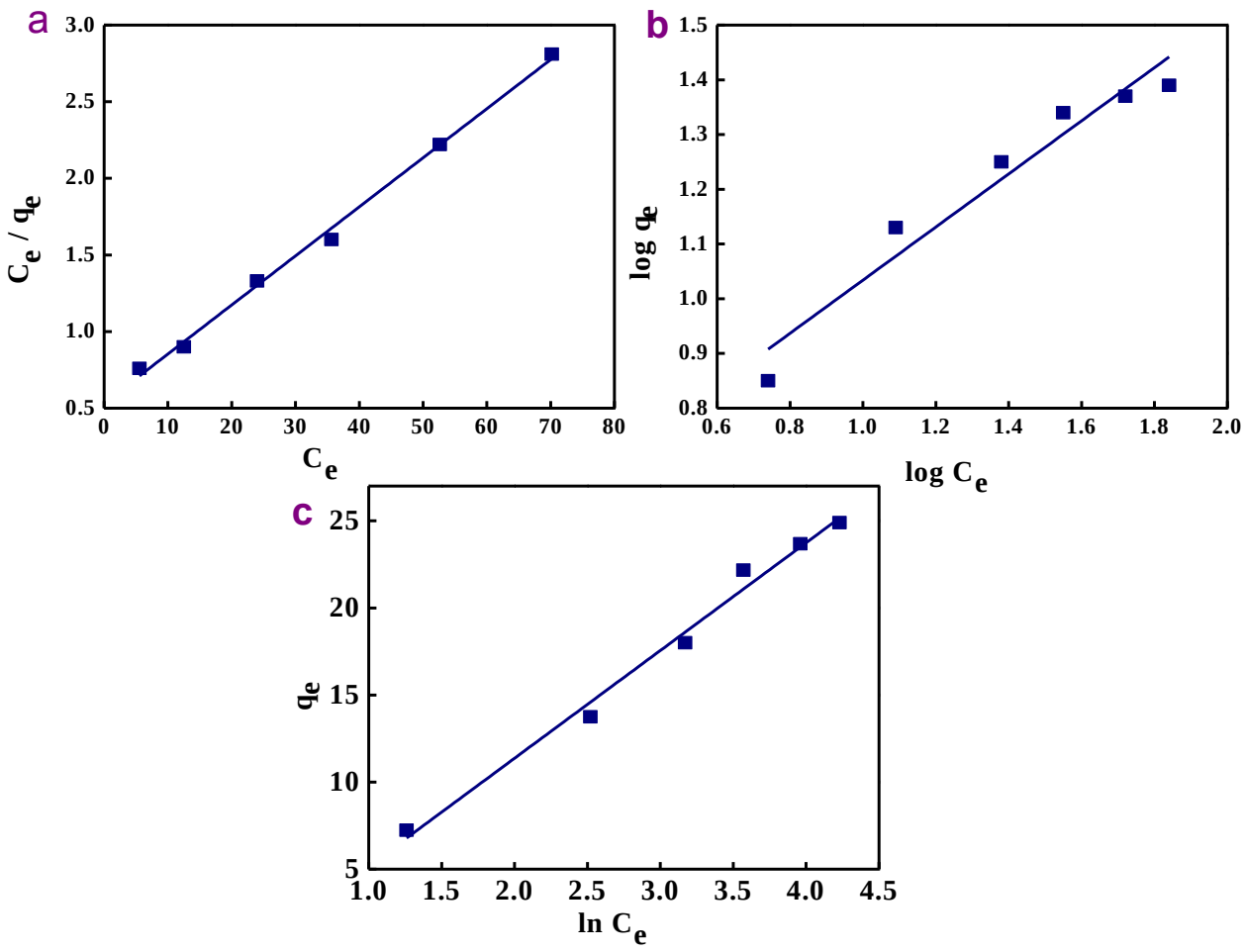

Fig.5 (a) Langmuir (b) Freundlich and (c) Tempkin isotherm models for adsorption of CB dye onto ST/PL(AA-*cl*-AAm) NHG

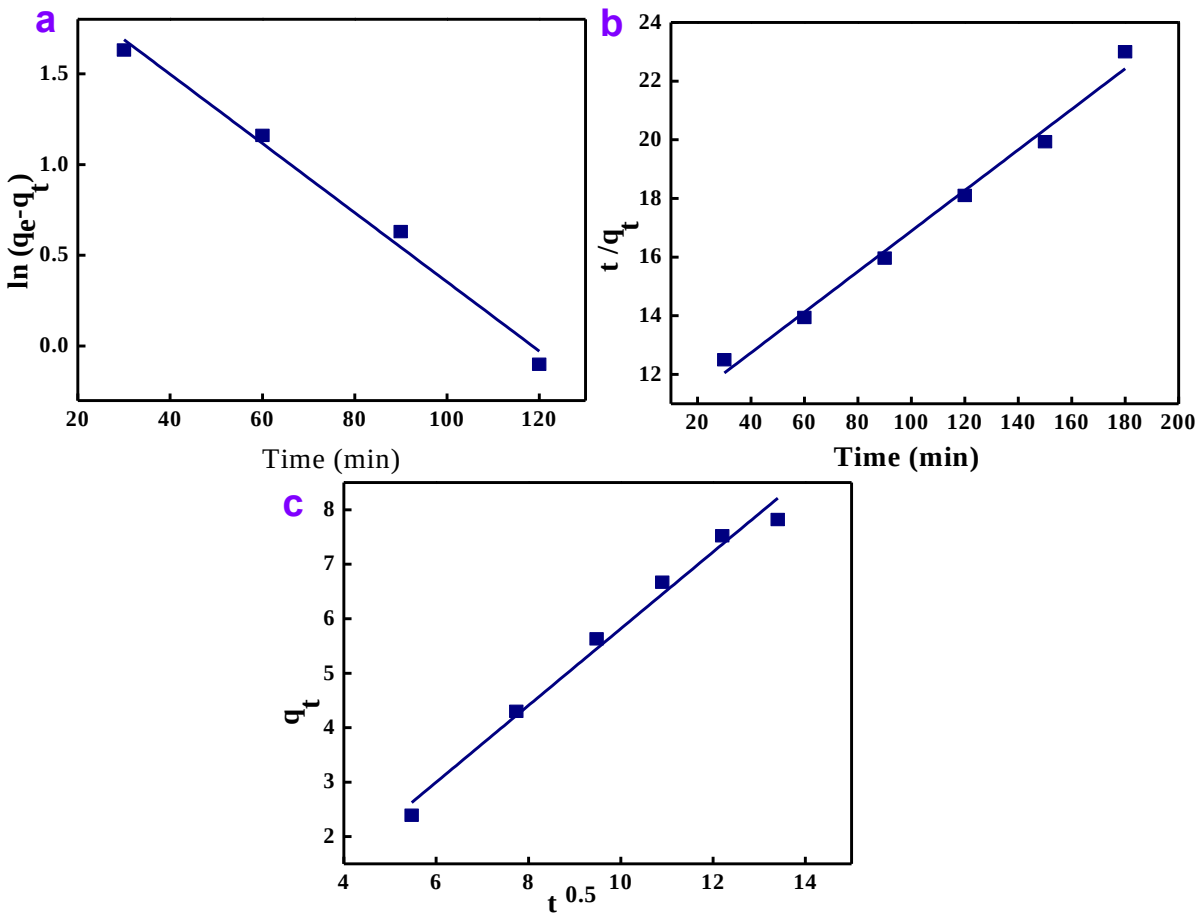

Fig.6 (a) Pseudo-first-order (b) Pseudo-second-order equation and (c) Weber-Morris model for adsorption quantity of CB dye onto ST/PL(AA-*cl*-AAm*)* NHG

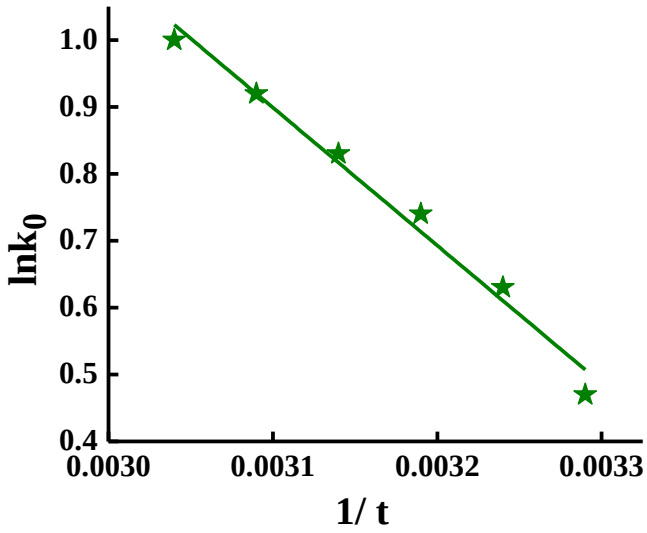

Fig.7 Van't Hoff plot for evaluating thermodynamic parameters for the removal of CB dye using ST/PL(AA-*cl*-AAm*)* NHG

Models		Isotherm constants		
Langmuir	Q_m (mg g^{-1})	K_L (L mg^{-1})	R_L	R^2
	31.24	0.056	0.47-0.12	0.99
Freundlich	n	K_f (mg g^{-1})		R^2
	2.05	3.53		0.93
Tempkin	B_1	K_T (L mg^{-1})		R^2
	6.18	0.850		0.98

Table 1 Isotherm parameters for the adsorption of CB onto ST/PL(AA-*cl*-AAm) NHG

Table 2. List of adsorbents available for the adsorption of CB dye

Adsorbents	Adsorption capacity q_m ($mg\ g^{-1}$)	References
Natural agalmatolite	11.29	(Sales et al. 2013)
Natural kaolinite	22.89	(Sales et al. 2013)
Fe_3O_4@C nanoparticles	11.22	(Ahmed et al. 2014)
NiO nanoparticles	11.21	(Abd-El-Aziz et al. 2016)
TiO_2/SiO_2	9.47	(Bujnakova et al. 2017)
PANI–$NiFe_2O_4$ magnetic nanocomposite	4.09	(Ansari et al. 2013)
Starch/poly(alginic acid-*cl*-acrylamide) nanohydrogel	31.24	Present study

Table 3. Values of various parameters of pseudo-first-order, pseudo-second-order, Weber-Morris and thermodynamics

	Plot parameters		
Pseudo-first-order	K_1 (min^{-1})	q_e (mg/g)	R^2
	0.019	10.62	0.983
Pseudo-second-order	K_2 (g mg^{-1} min^{-1})	q_e (mg/g)	R^2
	0.0047	14.46	0.986
Weber-Morris	k_{dif} (mg/(g $min^{0.5}$))	C	R^2
	0.704	-1.22	0.954
Thermodynamics	ΔG^0 (kJ mol^{-1})	ΔH^0 (kJ mol^{-1})	ΔS^0 (J mol^{-1} K^{-1})
	-1.25	17.15	60.64